molecules

MDPI

Article

Effects of *Juniperus communis* Cone Berry Extract and Solvent Fractions on Glycation of Human Serum Albumin

Arleta Dołowacka-Jóźwiak [1,*], Diana-Simona Tchiakpe-Antal [2,*], Alina Arabela Jojić [2], Katarzyna Wiglusz [3], Monika Gasztych [4], Bożena Karolewicz [1] and Ewa Żurawska-Płaksej [5]

[1] Department of Drug Form Technology, Faculty of Pharmacy, Wroclaw Medical University, Borowska 211a, 50-556 Wrocław, Poland
[2] Department of Pharmaceutical Botany, Faculty of Pharmacy, 'Victor Babeș' University of Medicine and Pharmacy Timișoara, 2 Eftimie Murgu Square, 300041 Timișoara, Romania
[3] Department and Institute of Basic Chemical Sciences, Faculty of Pharmacy, Wroclaw Medical University, Borowska 211a, 50-556 Wrocław, Poland
[4] Department of Physical Chemistry and Biophysics, Faculty of Pharmacy, Wroclaw Medical University, Borowska 211a, 50-556 Wrocław, Poland
[5] Department of Toxicology, Faculty of Pharmacy, Wroclaw Medical University, Borowska 211, 50-556 Wrocław, Poland
* Correspondence: arleta.dolowacka-jozwiak@umw.edu.pl (A.D.-J.); diana.antal@umft.ro (D.-S.T.-A.)

Abstract

Juniperus communis cone berries contain polyphenols that may influence protein glycation. We compared an ethanolic extract and five solvent fractions (10, 100, and 1000 µg/mL) in a human serum albumin (HSA; 40 mg/mL) model incubated with 30 or 300 mM glucose for 28 days at 37 °C (three independent incubations per condition). Fructosamine, advanced glycation end product (AGE)-associated fluorescence, and N^{ε}-(carboxymethyl)lysine (CML) were measured, and comparisons used the recorded protein-adjusted values for all endpoints. At 30 mM glucose, fructosamine responses decreased relative to the glucose control by 19.9%, 34.7%, and 62.0% with the diethyl ether fraction (F3) and by 37.7%, 39.8%, and 19.8% with the ethyl acetate fraction (F4) at 10, 100, and 1000 µg/mL, respectively. Fluorescence decreases could not be interpreted as equivalent reductions in AGE formation because some signals fell below the corresponding no-glucose backgrounds. The petroleum ether fraction (F2) decreased CML responses by 42.0%, 63.2%, and 77.3% at 30 mM glucose, whereas F4 decreased them by 2.1%, 60.4%, and 27.5% at 30 mM glucose. These preliminary findings prioritize F3 and F4 for validation of early glycation responses and F2 for CML assessment, with vehicle effects and assay interference remaining unresolved.

Keywords: *Juniperus communis*; human serum albumin; glycation; fructosamine; advanced glycation end products; carboxymethyllysine; hyperoside

Check for updates

Academic Editor: Irene Dini

Received: 25 October 2026
Revised: 21 November 2026
Accepted: 22 November 2026
Published: 26 November 2026

Copyright: © 2026 by the authors. Licensee MDPI, Basel, Switzerland. This article is an open access article distributed under the terms and conditions of the Creative Commons Attribution (CC BY) license.

1. Introduction

Protein glycation is a non-enzymatic process in which reducing sugars react with amino groups in proteins. The initial Schiff bases can rearrange into Amadori products, which subsequently undergo oxidation and fragmentation to generate advanced glycation end-products (AGEs) [1,2]. Reactive dicarbonyls, including methylglyoxal and glyoxal, provide additional routes to protein modification [3,4]. AGEs are chemically diverse: some are fluorescent, some form protein cross-links, and others modify individual amino-acid residues without either property [5]. This diversity is relevant both to their biological effects and to the choice of methods used to measure glycation.

Glycation can impair protein function through modification of amino-acid residues and formation of cross-links. In long-lived tissue proteins, these changes can alter the extracellular matrix; in circulating proteins, they can affect interactions with ligands [5,6]. Some AGE structures also activate the receptor for advanced glycation end-products (RAGE), linking protein modification to oxidative stress and inflammatory signalling. Sustained hyperglycaemia favours these reactions, which contribute to the pathophysiology of diabetes and its vascular complications. AGE-related damage is also relevant to diabetic kidney disease and age-related deterioration of renal function [7,8]. Preventing excessive glycation is therefore investigated as a means of preserving protein function and limiting damage associated with metabolic disease.

Glycation has particular relevance to ocular tissues, where long-lived proteins can accumulate modifications over time. Tezel et al. found increased AGE and RAGE immunoreactivity in the retina and optic nerve head of donor eyes with glaucoma [9]. Park and Kim reported oxidative stress and senescence after AGE exposure in cultured human trabecular meshwork cells [10]. These findings provide a rationale for investigating antiglycation approaches in ocular research. Albumin offers a tractable initial screening system, although effects in this soluble protein require confirmation in the relevant ocular cells or tissues.

Human serum albumin (HSA) transports endogenous and exogenous ligands and contributes to extracellular antioxidant defence. Glycation can alter its drug-binding properties [11], while glucose exposure and fatty-acid binding jointly affect thiol reactivity and antioxidant behaviour [12]. Changes in glycated HSA receptor interactions and immunogenicity have also been reported [13]. These functional consequences explain why a chemical glycation response should ultimately be assessed alongside preservation of protein function.

Plant polyphenols are investigated as glycation inhibitors because they may intercept reactive carbonyls, chelate metal ions or limit oxidative reactions involved in protein modification [14–16]. Edible plants and culinary herbs are potential dietary sources of such compounds. However, radical-scavenging activity alone cannot establish inhibition of glycation, whose several reaction pathways respond differently to individual polyphenols [17,18]. Studies of peppermint polyphenols and *Brassica* vegetables have combined glycation assays with chemical profiling and methylglyoxal-trapping measurements [19,20]. More recently, Sun et al. examined coffee-leaf extracts using fructosamine, CML, fluorescent products and dicarbonyl measurements in a bovine albumin–glucose model [21]. Such studies illustrate how composition and several complementary measurements can help identify the reactions affected by a plant preparation.

Juniperus communis L. pseudo-fruits, commonly called juniper berries or cone berries, are used as a spice and contain phenolic and terpenoid constituents [22,23]. Extraction conditions and solvent polarity influence the constituents recovered and the biological properties of the resulting preparations [24,25]. Dan et al. identified isoquercitrin, hyperoside, quercitrin and rutin in an ethanolic pseudo-fruit extract [26]. Jojić et al. subsequently found that the ethyl acetate-soluble fraction contained more total polyphenols and hyperoside than the *n*-butanol-soluble fraction, whereas the latter contained more rutin [27]. In the diethyl ether fraction, apigenin, protocatechuic acid and luteolin were the most abundant constituents quantified by targeted HPLC–MS [28].

Asgary et al. reported juniper antiglycation activity for essential oils from fruits and branchlets of *J. communis* subsp. *hemisphaerica* in haemoglobin and insulin assays [29]. These volatile preparations differ chemically from an ethanolic cone berry extract and its solvent fractions. Their activity therefore cannot be directly extrapolated to the effects of the preparations examined here on early and advanced products of HSA glycation.

HSA provides a controlled experimental model of glucose-induced modification of a physiologically relevant protein [30,31]. Fructosamine reflects early ketoamine formation [32], whereas fluorescence at selected excitation/emission wavelengths detects only fluorescent glycation-associated structures [33,34]. N^{ε}-(Carboxymethyl)lysine (CML) is a non-fluorescent lysine modification that can arise through glycoxidation and lipid-peroxidation pathways [35–37]. Measuring these products together helps distinguish an effect on early glycation from a change in selected advanced products. It also avoids treating a fluorescence decrease as a measurement of total AGE formation.

Plant constituents can also affect the analytical signals used to measure glycation, as shown by comparisons of extracts added during and after incubation [38], fluorescence screening of crude extracts [39] and spectroscopic studies of ligand binding to HSA [40]. We therefore included preparation-matched no-glucose backgrounds and interpreted fluorescence together with chemically distinct glycation readouts. These backgrounds do not replace vehicle-matched glucose controls.

This preliminary in vitro study compared an ethanolic extract of *J. communis* cone berries and five solvent fractions in a glucose-induced HSA glycation model. Fructosamine, AGE-associated fluorescence and CML were measured at three preparation concentrations, with aminoguanidine as a reference [41]. Published phytochemical profiles were used to interpret differences between preparations. The aim was to identify fractions for further chemical and biological evaluation and, if their activity is confirmed, for ophthalmic formulation development.

2. Results

2.1. Control Responses

Three independent incubations were performed per condition, and results are presented as mean ± SD. Glucose-containing controls showed higher recorded responses than HSA-only samples (Table 1). The difference between 30 and 300 mM glucose was most pronounced for fructosamine and was also apparent at both fluorescence wavelength pairs. CML measurements are treated as exploratory. Figures 1 and 2 show the recorded protein-adjusted responses as percentages of the corresponding glucose control (100%). A reduction of x% corresponds to a plotted response of $(100 - x)$%. Preparation-matched no-glucose backgrounds are considered separately in Figures 3 and S1. With three independent incubations per condition, treatment/control comparisons are presented descriptively as the mean ± SD of within-incubation percentages.

Table 1. Control assay responses in HSA incubated with and without glucose. Mean ± SD ($n = 3$).

Measurement	No Glucose	30 mM Glucose	300 mM Glucose
Fluorescence, 335 nm excitation (AU)	23.50 ± 1.50	48.07 ± 1.01	120.18 ± 2.27
Fluorescence, 370/440 nm (AU)	34.19 ± 1.29	46.28 ± 1.45	128.10 ± 2.15
Fructosamine (nmol/mg protein)	14.67 ± 0.58	50.28 ± 2.06	332.98 ± 4.33
CML (ng/mg protein)	22.10 ± 1.15	49.07 ± 0.89	80.08 ± 5.09

Values are reported on the recorded protein-adjusted scales; the limitations of cross-endpoint normalization are described in Section 4.4. AU denotes arbitrary units after fluorescence adjustment. The three CML controls underlying the 300 mM summary could not be linked to the within-incubation controls used for Figure 1D (Section 4.7).

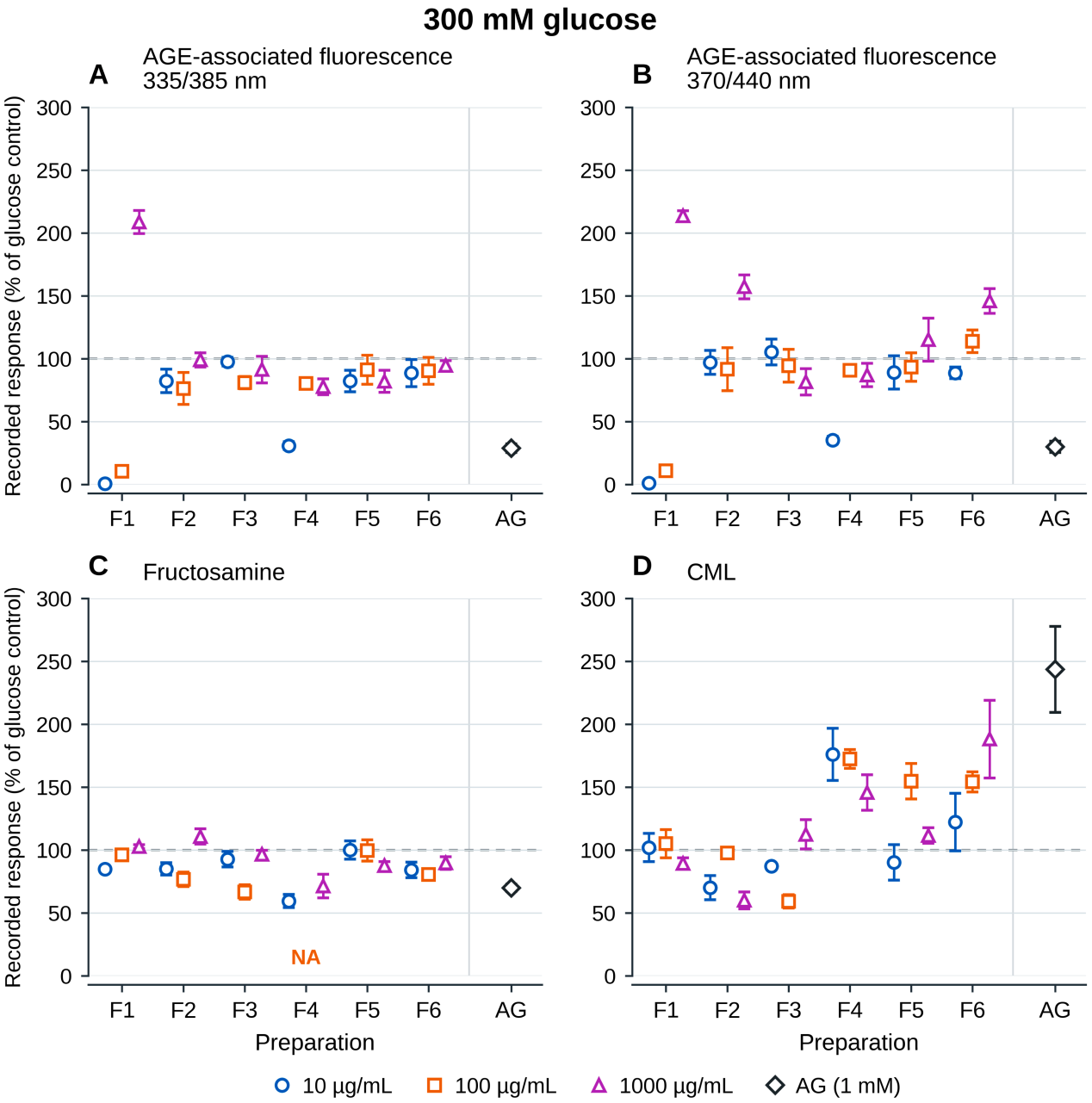

Figure 1. Recorded responses in the human serum albumin (HSA)–glucose model at 300 mM glucose. Panels (**A**,**B**) show AGE-associated fluorescence in the 335 nm excitation and 370/440 nm channels, respectively. Panel A uses the compiled data label (see Section 4.6). Panels (**C**,**D**) show fructosamine and CML, respectively. All percentages of the glucose control were calculated from the recorded protein-adjusted readouts (normalization limitations: Section 4.4). The underlying units were AU (arbitrary units) for adjusted fluorescence, nmol/mg protein for fructosamine and ng/mg protein for CML. Symbols and whiskers show mean ± SD of within-experiment treatment/control percentages from three independent incubations ($n = 3$). The dashed line denotes the glucose control (100%). Colours and symbol shapes identify preparation concentrations (10, 100 and 1000 µg/mL); black diamonds denote 1 mM aminoguanidine (AG). F1, crude ethanolic extract; F2, petroleum ether fraction; F3, diethyl ether fraction; F4, ethyl acetate fraction; F5, *n*-butanol fraction; F6, aqueous fraction. Plotted response (%) = 100 − reduction (%) reported in Table S1B. For F4 at 100 µg/mL, NA marks the unavailable fructosamine result. Table S1B identifies the record used for the other endpoints. CML responses are exploratory. Fluorescence decreases do not quantify inhibition of total AGE formation.

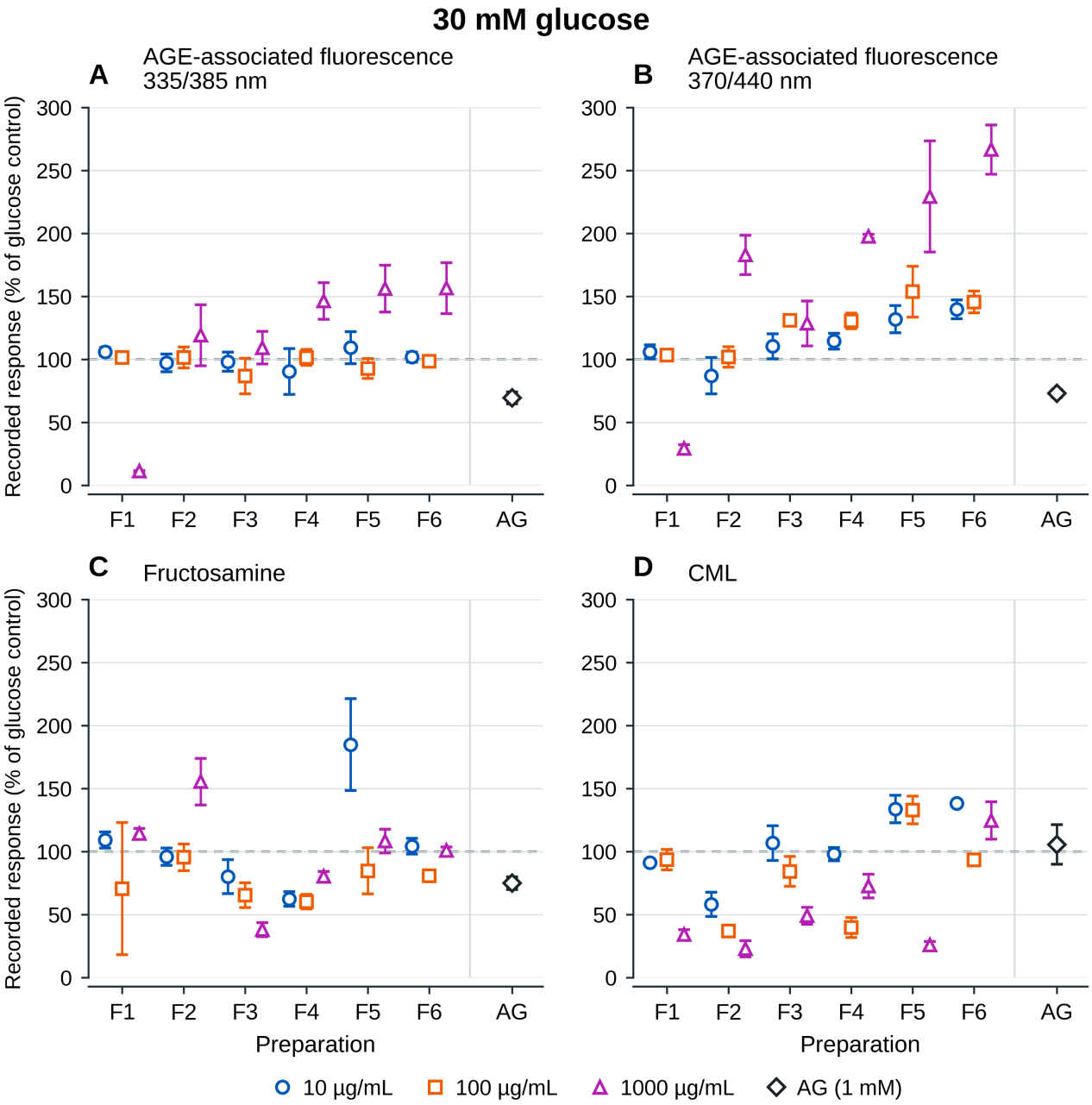

Figure 2. Recorded responses in the human serum albumin (HSA)–glucose model at 30 mM glucose. Panels (**A**,**B**) show AGE-associated fluorescence in the 335 nm excitation and 370/440 nm channels, respectively. Panel (**A**) uses the compiled data label (see Section 4.6). Panels (**C**,**D**) show fructosamine and CML, respectively. All percentages of the glucose control were calculated from the recorded protein-adjusted readouts (normalization limitations: Section 4.4). The underlying units were AU (arbitrary units) for adjusted fluorescence, nmol/mg protein for fructosamine and ng/mg protein for CML. Symbols and whiskers show mean ± SD of within-experiment treatment/control percentages from three independent incubations ($n = 3$). The dashed line denotes the glucose control (100%). Colours and symbol shapes identify preparation concentrations (10, 100 and 1000 µg/mL); black diamonds denote 1 mM aminoguanidine (AG). F1, crude ethanolic extract; F2, petroleum ether fraction; F3, diethyl ether fraction; F4, ethyl acetate fraction; F5, *n*-butanol fraction; F6, aqueous fraction. Plotted response (%) = 100 − reduction (%) reported in Table S1A. CML responses are exploratory. Fluorescence decreases do not quantify inhibition of total AGE formation.

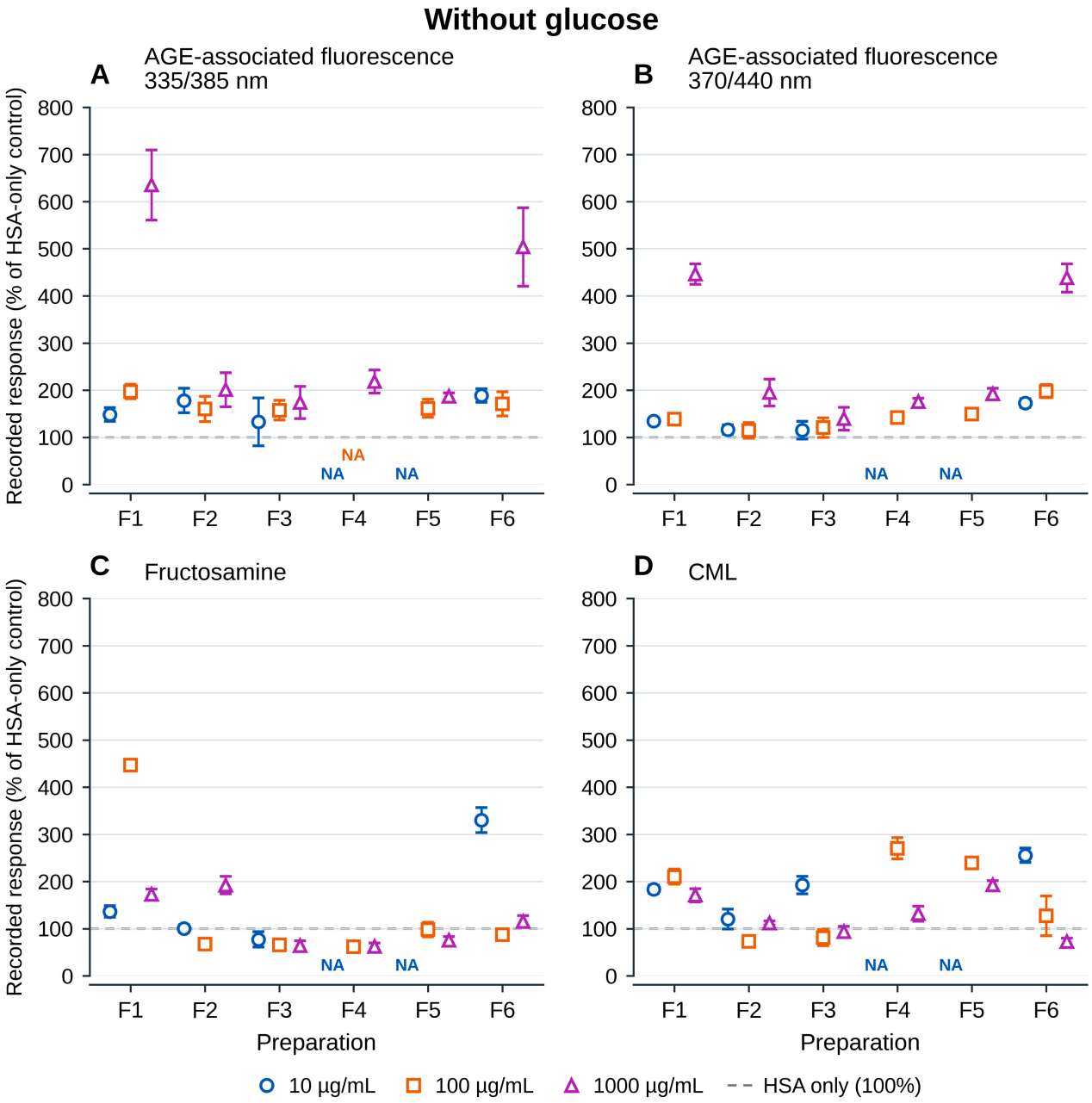

Figure 3. Recorded responses of human serum albumin (HSA) incubated with juniper preparations without added glucose. Panels (**A**,**B**) show fluorescence in the 335 nm excitation and 370/440 nm channels, respectively. Panel (**A**) uses the compiled data label (see Section 4.6). Panels (**C**,**D**) show fructosamine and CML, respectively. All percentages of the HSA-only control were calculated from protein-adjusted readouts. The underlying units were AU (arbitrary units) for adjusted fluorescence, nmol/mg protein for fructosamine and ng/mg protein for CML. Symbols and whiskers show mean ± SD of within-experiment percentages from three independent incubations ($n = 3$). The dashed line denotes the HSA-only control (100%). Colours and symbol shapes identify preparation concentrations (10, 100 and 1000 µg/mL). F1, crude ethanolic extract; F2, petroleum ether fraction; F3, diethyl ether fraction; F4, ethyl acetate fraction; F5, *n*-butanol fraction; F6, aqueous fraction. NA denotes an unavailable complete recorded triplet. These measurements characterize assay backgrounds and do not measure inhibition of glycation; CML responses remain exploratory.

2.2. Responses at 300 mM Glucose

At 300 mM glucose, the F4 fructosamine response was lower by 40.6 ± 5.3% at 10 µg/mL and 28.7 ± 9.4% at 1000 µg/mL; the result at 100 µg/mL was unavailable (Figure 1C;

Table S1B). F3 showed reductions of 7.4 ± 6.2%, 33.4 ± 5.8% and 3.5 ± 3.3% at 10, 100 and 1000 μg/mL, respectively. F2 showed reductions at 10 and 100 μg/mL but a 10.7 ± 6.1% increase at 1000 μg/mL. F1 showed its largest reduction at 10 μg/mL (15.3 ± 0.6%). F5 showed minimal changes at 10 and 100 μg/mL and a 12.4 ± 3.2% reduction at 1000 μg/mL, whereas the F6 reductions ranged from 10.4% to 19.5%. The calibration range was 0–10 mmol/L, and the first-incubation glucose-control estimate of 9.46 mmol/L was within this range. Three first-incubation treatment estimates (F1 at 100 μg/mL, F2 at 1000 μg/mL and F3 at 1000 μg/mL) exceeded 10 mmol/L and were obtained by extrapolation; comparisons for these conditions are presented descriptively (Section 4.5). The F4 responses at 10 and 1000 μg/mL were lower than the glucose control in each of the three incubations, so their direction did not depend on the first incubation (Table S1B).

Fluorescence showed a different concentration-dependent pattern (Figure 1A,B; Table S1B). At 10 μg/mL, F1 showed reductions of 99.5 ± 0.1% in the 335 nm excitation channel and 99.1 ± 0.1% at 370/440 nm. At 100 μg/mL, the corresponding reductions were 89.6 ± 1.4% and 89.1 ± 1.2%; at 1000 μg/mL, both signals exceeded the glucose control. F4 at 10 μg/mL showed reductions of 69.3 ± 3.1% and 64.8 ± 2.9%, respectively, with smaller reductions at 100 and 1000 μg/mL. F2, F3, F5 and F6 showed smaller reductions in the 335 nm excitation channel and variable responses at 370/440 nm, including values above the control for F2, F5 and F6 at 1000 μg/mL. The F1 signals at the two lower concentrations were also below the corresponding no-glucose backgrounds (Figure 3). These optical decreases cannot be equated with inhibition of total AGE formation.

The CML pattern differed from those of fructosamine and fluorescence (Figure 1D; Table S1B). F3 showed its largest reduction at 100 μg/mL (40.9 ± 5.4%), whereas F2 showed reductions of 29.9 ± 9.6%, 2.5 ± 2.7% and 40.1 ± 6.7% at 10, 100 and 1000 μg/mL, respectively. F4 responses exceeded the glucose control at all three concentrations, reaching 176.0%, 172.4% and 145.7% of control, respectively. F5 responses exceeded control at 100 and 1000 μg/mL, and F6 responses exceeded control at all three concentrations. F1 showed no consistent reduction across concentrations. These observations describe recorded assay responses and do not establish promotion or inhibition of CML formation.

Aminoguanidine (AG; 1 mM) showed a fructosamine reduction of 30.1 ± 2.9% and fluorescence reductions of 71.2 ± 3.4% and 70.2 ± 4.5% in the 335 nm excitation and 370/440 nm channels, respectively. Its recorded CML response reached 243.5 ± 34.1% of the glucose control. This discordant CML result requires analytical validation.

2.3. Responses at 30 mM Glucose

At 30 mM glucose, responses differed among preparations and endpoints (Figure 2; Table S1A). F3 showed progressively greater fructosamine reductions of 19.9 ± 13.5%, 34.7 ± 9.9% and 62.0 ± 5.5% at 10, 100 and 1000 μg/mL, respectively (Figure 2C). Its CML reduction reached 51.0 ± 6.7% at 1000 μg/mL (Figure 2D). In contrast, fluorescence in the 335 nm excitation channel showed small mean reductions at 10 and 100 μg/mL and exceeded control at 1000 μg/mL; at 370/440 nm, responses exceeded control at all three concentrations (Figure 2A,B).

F4 showed fructosamine reductions of 37.7 ± 5.8%, 39.8 ± 5.7% and 19.8 ± 4.0% at 10, 100 and 1000 μg/mL, respectively (Figure 2C). The corresponding plotted responses were 62.3%, 60.2% and 80.2% of the glucose control; the largest mean decreases therefore occurred at the two lower concentrations. The CML reductions were 2.1 ± 5.2%, 60.4 ± 7.9% and 27.5 ± 9.4%, respectively (Figure 2D). Fluorescence showed no parallel pattern: only the mean response in the 335 nm excitation channel at 10 μg/mL was below control, whereas the 370/440-nm responses exceeded control at every concentration (Figure 2A,B).

F2 showed progressively greater CML reductions of 42.0 ± 9.6%, 63.2 ± 4.6% and 77.3 ± 6.4% at 10, 100 and 1000 µg/mL, respectively (Figure 2D). At 1000 µg/mL, its fructosamine and both fluorescence responses exceeded the glucose control. F5 showed a similar endpoint discrepancy at 1000 µg/mL: the CML response was lower by 74.3 ± 2.9%, while fructosamine and both fluorescence responses exceeded control (Figure 2A–D).

F1 showed variable fructosamine responses, including a mean reduction of 29.5 ± 52.4% at 100 µg/mL. At 1000 µg/mL, its fluorescence responses were markedly lower at both wavelength pairs, despite an increased fructosamine response. F6 showed no consistent reduction across all endpoints. AG showed a fructosamine reduction of 25.1 ± 5.0% and fluorescence reductions of 30.7 ± 4.7% and 27.1 ± 3.2% in the 335 nm excitation and 370/440 nm channels, respectively; its CML response was 105.5 ± 15.7% of control (Figure 2).

2.4. Background Signals

HSA samples incubated with a juniper preparation without added glucose showed fluorescence, fructosamine and CML responses that differed from those of HSA-only samples (Figure 3). These responses are expressed relative to HSA-only controls, whereas Figures 1 and 2 use the corresponding glucose controls. F1 at 1000 µg/mL showed particularly high fluorescence backgrounds (635.1 ± 74.6% in the 335 nm excitation channel and 446.2 ± 21.5% at 370/440 nm), and F6 at 1000 µg/mL gave backgrounds of similar magnitude (Figure 3A,B). In the fructosamine assay, backgrounds were elevated for F1 at 100 µg/mL and F6 at 10 µg/mL, whereas F3 and F4 at 100 and 1000 µg/mL gave values below the HSA-only control (Figure 3C). Complete recorded no-glucose triplets were unavailable for some conditions, which are marked NA in Figure 3.

Subtraction of matched preparation-containing no-glucose backgrounds produced a separate set of calculated reductions (Figure S1). For F1 at 10 µg/mL and 300 mM glucose, the 370/440 nm readings were 1.12 ± 0.16 AU with glucose and 45.99 ± 0.98 AU without glucose. The corresponding controls without F1 were 128.10 ± 2.15 and 34.19 ± 1.29 AU. Averaging the reductions after matched subtraction within each incubation gave 135.2% in the 335 nm excitation channel and 147.8% at 370/440 nm (135% and 148% in Figure S1). Calculated fluorescence reductions reached 1248% for F1 at 1000 µg/mL and 30 mM glucose at 370/440 nm, and the calculated CML reduction reached −244% for F6 at 1000 µg/mL and 300 mM glucose. With a positive net control signal, a negative net treatment signal gives a calculated reduction above 100%; a net treatment signal above the net control gives a negative reduction. These values characterize the sensitivity of assay responses to subtraction of separately measured backgrounds. They cannot be interpreted as proportional changes in glycation or AGE formation because background contributions may not remain additive in glucose-containing samples.

3. Discussion

The preparations produced different responses across the measured endpoints. At 30 mM glucose, F3 showed progressively greater fructosamine reductions as its concentration increased, whereas F4 showed its largest decreases at 10 and 100 µg/mL (Figure 2C; Table S1A). The interpretation of F3 as a candidate for further investigation of early glycation is therefore focused on the 30 mM condition. F2 showed progressively lower CML responses at 30 mM glucose, while F4 gave lower CML responses at 30 mM and higher responses at 300 mM glucose (Figures 1D and 2D; Tables S1A and S1B). The lower F4 fructosamine response at 30 mM glucose was also present before protein normalization (Table S2). These observations identify distinct conditions for chemical validation; they do not establish a common mechanism of AGE inhibition.

Fructosamine reflects early ketoamine formation [32], fluorescence detects selected glycation-associated fluorophores [33,34], and CML is a non-fluorescent lysine modification with several formation routes [35–37]. Differences between these endpoints may consequently reflect effects on different reactions, as well as analytical interference. For example, F5 at 1000 μg/mL and 30 mM glucose gave a lower CML response while fructosamine and both fluorescence responses exceeded the glucose control (Figure 2; Table S1A). Such discordance limits interpretation of any single marker as evidence of broad antiglycation activity.

In our earlier 28-day albumin study, an ethyl acetate fraction of *Reynoutria sachalinensis* also lowered the NBT-based fructosamine response [42]. That experiment used a combined glucose–fructose challenge and a chemically different fraction, so its effect size cannot be transferred to the present INT assay. Asgary et al. examined steam-distilled juniper essential oils in haemoglobin and insulin assays over 48 h [29]. These oils consisted predominantly of volatile monoterpenes and were tested as mixtures; their activity cannot be attributed to the non-volatile flavonoids identified in the present ethanol-derived preparations. Sun et al. reported decreases in fructosamine, CML, fluorescent products and reactive dicarbonyls in a coffee-leaf BSA–glucose model [21], whereas the present fractions showed less agreement between endpoints. The additional measurements of oxidation and protein structure used in a prunin–HSA study illustrate how such differences can be investigated [43].

3.1. Polyphenolic Constituents and Potential Mechanisms

The published profiles identify isoquercitrin, hyperoside, quercitrin and rutin in the crude extract of juniper cone berries (F1) [26]. Upon fractionation with solvents of increasing polarity, the sub-extracts acquired different compositions according to the solubility of their constituents. The ethyl acetate fraction F4 had the highest total phenolic content among the F4 and F5 fractions compared in the published study: 361.08 ± 17.72 mg chlorogenic acid equivalents (CAE)/g extract, versus 104.73 ± 10.03 mg CAE/g extract for the *n*-butanol fraction. F4 was particularly rich in hyperoside and also contained protocatechuic acid and apigenin [27]. The diethyl ether fraction F3 contained less total phenolics (114.22 ± 5.35 mg CAE/g extract), with apigenin, protocatechuic acid and luteolin as its three highest quantified constituents [28]. In the present study, the F4 fructosamine response was most pronounced at the two lower concentrations at 30 mM glucose, whereas F3 showed a concentration-related fructosamine decrease under this condition. F3 also gave a lower CML response at 100 μg/mL and 300 mM glucose (Figure 1D; Table S1B). These compositional and response differences support investigating whether F3 and F4 affect different reactions in early and advanced glycation.

Other flavonoids identified in juniper, including hyperoside and related glycosides, have also been examined directly in antiglycation studies. Hyperoside was investigated among the phenolic constituents of *Cistus* × *incanus*, while hyperoside and isoquercitrin were identified among inhibitors from lotus leaves [44,45]. The catechol-bearing structures of luteolin, hyperoside and protocatechuic acid provide a chemical basis for radical scavenging and metal interactions that may limit oxidative steps in glycation. Antiglycation and antioxidant activities of related polyphenols have been demonstrated for eriodictyol, butein and sulfuretin [46,47]. Isoquercitrin has also been studied with β-lactoglobulin and ovalbumin using mass spectrometry and protein-interaction measurements [48,49]. These findings support testing the glycosides at concentrations established by chemical analysis of F4. Glycosylation changes albumin association [50], so the response of a whole fraction cannot be assigned to hyperoside alone or predicted quantitatively from quercetin.

Apigenin and luteolin are flavone aglycones with evidence of activity at several stages of glycation. Apigenin scavenges methylglyoxal, a reactive α-dicarbonyl intermediate, through adduct formation, thereby reducing its availability for protein modification [51].

Studies of flavone aglycones have identified mono- and di-methylglyoxal adducts of apigenin and luteolin, with C6 and C8 of the A-ring as proposed sites of addition [19]. Luteolin inhibited glyoxal-induced AGE formation and aggregation in an HSA model [52] and was identified as an AGE inhibitor in olive leaves [53]. Grzegorczyk-Karolak et al. reported an 85.4% reduction in their AGE-formation readout with isolated luteolin at 100 µg/mL [54]. These observations provide a mechanistic rationale for examining apigenin- and luteolin-containing F3. However, the activity of isolated compounds in different protein and glycating-agent systems is not a potency estimate for the whole fraction, and the present CML response cannot be assigned specifically to apigenin–methylglyoxal adduct formation.

Protocatechuic acid, a phenolic acid present in F3 and F4, offers a further mechanism for affecting protein glycation. In a BSA–glucose model, it inhibited the formation of early Amadori products, fluorescent AGEs and CML. Tagliazucchi et al. identified protein–phenolic adducts by mass spectrometry and proposed binding to lysine through a metal-catalysed oxidative mechanism [55]. Occupation of glycation-prone amino groups can reduce their availability for glucose attachment. This supports investigating direct protein interactions alongside carbonyl trapping, while recognising that protein modification by a phenolic compound does not itself establish preservation of albumin function.

The presence of hyperoside, apigenin, luteolin and protocatechuic acid therefore supports investigating complementary antiglycation mechanisms in the juniper fractions. Quercetin, the aglycone of hyperoside and several other juniper glycosides, provides additional context through its reported methylglyoxal trapping, metal chelation and reactive oxygen species scavenging [56]. Structure–activity comparisons demonstrate that flavonoid substitution influences glycation responses [57]. In an HSA–glucose study that included apigenin and luteolin, hydroxylation at C4′ and a C2–C3 double bond were associated with greater antiglycation potential, whereas methylation of the C3 hydroxyl reduced the effect [58]. Rutin can also form adducts with methylglyoxal and glyoxal [59]. Together, these reactions provide plausible routes for reducing carbonyl stress by limiting the availability of reactive dicarbonyls [60] and for affecting oxidative steps leading to AGE formation. CML also arises through other pathways, including oxidative cleavage of Amadori products [35–37], so methylglyoxal trapping alone cannot explain its response. Carbonyl trapping, metal chelation and individual constituent contributions remain hypotheses in the present incubations.

F5, the *n*-butanol-soluble fraction, contained more rutin than F4 in the published analysis [27], yet its fructosamine response did not reproduce the F4 pattern. Studies comparing rutin and quercetin, and work with glycated low-density lipoprotein, likewise demonstrate the importance of the protein, glycating agent and experimental conditions [61,62]. Equal dry-mass concentrations of F1, F3, F4 and F5 consequently provide different molar exposures to individual compounds. Mixture composition may therefore matter as much as the presence of rutin alone. Interpretation was focused on these chemically characterised preparations; specific active constituents were not assigned to F2.

The antioxidant potential of juniper berry extracts may contribute to their antiglycation activity because radical scavenging can limit oxidative steps of AGE formation. Our earlier research related the antioxidant properties of the fractions to their phytochemical profiles: the F4/F5 study reported stronger DPPH radical-scavenging activity for F4, whereas the F3 study described its DPPH assessment as exploratory [27,28]. Radical scavenging is a general property of flavonoids and phenolic acids bearing phenolic hydroxyl groups. Compounds abundant in juniper berries, including the flavones apigenin and luteolin, flavonols such as quercetin and rutin, and protocatechuic acid, are recognised contributors [63,64]. Their coexistence provides a basis for complementary actions and a hypothesis of synergy within the mixture; synergy was not tested in this study. Antioxidant capacity alone cannot

establish inhibition of HSA glycation. The ethanol-derived preparations were examined as a common fractionation series linked to these chemical profiles. A matched methanolic extract was not included, so the results do not identify an optimal extraction solvent.

3.2. Interpretation of Fluorescence and CML

The large F1 fluorescence decreases require particular caution. At 300 mM glucose, the signals at 10 and 100 µg/mL were below the corresponding no-glucose backgrounds; at 30 mM glucose, the highest F1 concentration also produced substantial preparation-containing backgrounds (Figures 1–3). Fluorescence may combine glycation-associated emission, intrinsic preparation fluorescence and preparation–protein interactions. Subtraction assumes that the background contribution remains additive in the glucose-containing sample. The calculated values outside the 0–100% range in Figure S1 show why the resulting reductions cannot be equated with proportional inhibition of AGE formation.

Séro et al. demonstrated interference in crude-extract screening in two AGE-associated fluorescence channels using a BSA–ribose model [39]. Sample autofluorescence, attenuation of excitation or emission light, and constituent–HSA interactions are plausible contributors to the present F1 pattern. Inner-filter correction requires absorbance at the relevant excitation and emission wavelengths and information about optical geometry [65]. Protein normalization using A_{280} does not itself correct these effects or exclude an absorbance contribution from fraction constituents to the protein estimate.

Usacheva et al. found that the solvent affected curcumin binding to HSA, while the quercetin binding constant was similar across the solvent conditions tested [40]. Extract-only spectra, dilution-linearity tests and absorbance measurements would help resolve optical contributions. Ishikawa et al. combined coaddition and postaddition experiments with an additional lysozyme-dimer assay [38]. Their approach distinguishes effects during glycation from effects on preformed glycation-related modifications and provides a useful framework for examining the juniper preparations.

CML responses differed from fructosamine and fluorescence. In particular, aminoguanidine at 300 mM glucose reached 243.5% of the glucose-control CML value, and F4 responses changed direction between the two glucose conditions (Figures 1D and 2D). Aminoguanidine is an established carbonyl-reactive reference compound [41,60], but CML can also arise by oxidative cleavage of Amadori products [35,36], a route that does not depend on free dicarbonyls. In the presence of transition metals, aminoguanidine can generate hydrogen peroxide and inactivate catalase [66], and it increased Cu(II)-dependent dicarbonyl generation by glycated albumin [67]. Such pro-oxidant activity during a 28-day incubation at 300 mM glucose could favour glycoxidative CML formation. This discordance therefore warrants investigation of the analytical system. The recorded CML ratios cannot be assigned to promotion or inhibition of CML formation without independently verifying assay performance in the preparation-containing matrix. CML samples were applied undiluted (50 µL per well; sample dilution factor = 1).

Spike recovery and dilution parallelism are needed to support quantitative CML comparisons in this matrix. An independent chemically selective measurement, such as LC–MS/MS of defined CML adducts, would help distinguish a change in glycation chemistry from a change in immunoassay response [68]. The lower F2 CML responses at 30 mM glucose therefore remain an exploratory observation rather than evidence of established protection against advanced glycation.

3.3. Biological Relevance

The functional relevance of a glycation response depends on preservation of the protein. Glycation can alter albumin drug binding [11], and glucose exposure together with

fatty-acid binding affects thiol reactivity [12]. Croes et al. reported altered receptor interactions and immunogenicity of glycated HSA [13], whereas Junho et al. found limited inflammatory effects of endotoxin-free AGE-modified albumin in their endothelial and neutrophil models [69]. A decrease in an analytical marker alone cannot predict a uniform biological benefit.

The cellular effects of the four polyphenols highlight a further aspect of their biological relevance. Hyperoside, a flavonol glycoside, downregulated RAGE expression, inhibited AGE-induced JNK activation and apoptosis, and promoted viability in AGE-stimulated ECV304 cells [70]. Apigenin and its methylglyoxal adduct attenuated AGE-induced oxidative stress and inflammatory responses in human umbilical vein endothelial cells [51]. The di-methylglyoxal apigenin adduct also reduced RAGE mRNA and protein expression, reactive oxygen species and proinflammatory mediators, including TNF-α, IL-1 and IL-6, in RAW 264.7 macrophages; related anti-inflammatory effects were observed in macrophage–endothelial cocultures [71]. These studies support considering both direct reactions with glycation intermediates and the biological activity of the resulting adducts. They provide a rationale for subsequent cell-based evaluation of F3 and F4 after chemical validation. RAGE and JNK signalling concern responses to preformed AGEs and were absent from the present acellular HSA incubation; they cannot directly explain the recorded fructosamine or CML responses.

Animal studies add context to the potential downstream effects of these constituents. Protocatechuic acid reduced glycation-related and oxidative markers in D-galactose-treated mouse brain [72] and lowered AGE/RAGE-associated changes in the retina of diabetic rats [73]. The retinal findings are relevant to the proposed ocular direction of further research. For luteolin, Huang et al. identified AGE–RAGE signalling and TGF-β, IL-1β and PPARG among the pathways and targets implicated by their network analysis. Their diabetic mouse study supported effects involving AMPK/NLRP3/TGF-β signalling, inflammation and renal fibrosis [74]. These findings extend the rationale beyond direct glycation chemistry, but include metabolic and cellular processes absent from the albumin model and do not establish efficacy of the juniper fractions. The glaucoma-associated tissue and cell findings [9,10] support later ocular studies; intraocular pressure, retinal function and glaucoma progression were not assessed here.

The earlier HET-CAM evaluation concerned a crude juniper extract [26]. It does not establish ocular tolerability of the individual solvent fractions. The F3 publication also reported concentration-related effects on HaCaT keratinocyte viability [28], supporting the need for fraction-specific safety testing. Formulation, route and local exposure must be considered separately from dietary use; oral polyphenol availability depends on absorption and metabolism [75–77]. No ophthalmic dose can be inferred from the present in vitro concentrations.

3.4. Study Limitations

Three independent incubations per condition provide descriptive estimates of variability [78] but do not support formal statistical inference; differences are therefore reported descriptively. At 300 mM glucose, three treatment estimates exceeded the upper calibrator (10 mmol/L) and were extrapolated; these comparisons are descriptive. All relative responses used the recorded protein-adjusted values. For F4 at 10 and 100 µg/mL and 30 mM glucose, the fructosamine response was lower in all three incubations both before adjustment and after a separate A_{280}-based recalculation. The recalculation used a provisional assignment of A_{280} records (Section 4.4) and changed the magnitude and variability of the reductions. It supports a descriptive sensitivity comparison rather than verification

of a common protein denominator. Fraction-matched controls for absorbance at 280 nm were unavailable.

The preparations were dosed in DMSO/PBS, as in our earlier albumin study [42], with estimated final DMSO concentrations of 0.01875%, 0.1875% and 1.875% (*v*/*v*). Grigoryan and Shilajyan examined intrinsic HSA fluorescence at 5% and 20% DMSO during short exposures [79]. Those conditions do not establish the absence of vehicle effects in a 28-day glycation incubation. All preparations shared the same final DMSO concentration at a given dose, permitting descriptive comparisons under a shared vehicle condition. This does not isolate the vehicle contribution or exclude interactions between DMSO and preparation constituents. At 10 µg/mL (0.01875% DMSO), F4 showed a 37.7% fructosamine decrease, whereas F1, F5 and F6 did not, and the F4 response was similar at 10 and 100 µg/mL despite a tenfold difference in DMSO concentration (Table S1A). Preparation-matched no-glucose backgrounds cannot isolate the effect of DMSO during glycation; glucose-containing controls matched to each final vehicle concentration are required to attribute the responses to fraction constituents.

The INT assay measures tetrazolium-reducing activity, and preparation-dependent effects on its colour reaction or optical readout remain possible after blank correction. No-glucose backgrounds show that some preparations alter the readout independently of added glucose (Figure 3C). For F4 at 100 µg/mL, the background was 61.4% of the HSA-only value, about 5.7 nmol/mg protein below that control (14.67 nmol/mg protein; Table 1), compared with an approximately 20 nmol/mg decrease relative to the 30 mM glucose control (39.8% of 50.28 nmol/mg protein). Under an additive-background assumption, the former would account for less than one-third of the latter; however, additivity has not been established, and this calculation cannot exclude interference. The lower CML response at this concentration (60.4 ± 7.9%; Table S1A) is a separate exploratory immunoassay observation and does not provide validated confirmation of the INT result because CML matrix validation is also outstanding. Post-addition of the fraction to previously glycated HSA and independent quantification of a defined Amadori product would help distinguish altered glycation from an effect on the assay [38,68]. These tests were not performed here. Carbonyl trapping, metal chelation, reactive oxygen species, individual constituent concentrations during incubation and protein function were not measured. Published profiles identify plausible mechanisms and compounds for testing, without demonstrating which caused the present fraction responses.

4. Materials and Methods

4.1. Reagents

Human serum albumin (HSA; Fraction V, purity ≥98%, approximate molecular mass 67 kDa), D-(+)-glucose, aminoguanidine hydrochloride (>98%), sodium azide, and dimethyl sulfoxide (DMSO) were obtained from Sigma-Aldrich (St. Louis, MO, USA). Petroleum ether, diethyl ether, ethyl acetate, and *n*-butanol used for sequential liquid–liquid partitioning were purchased from Sigma-Aldrich. Other reagents were of analytical grade, and ultrapure water was used throughout.

4.2. Plant Material and Preparations

Dried cone berries of *Juniperus communis* L. (Cupressaceae) were purchased as loose whole berries from Stef Mar (Râmnicu Vâlcea, Romania; product code 6422579000788). Prof. Diana-Simona Tchiakpe-Antal authenticated the material by macroscopic and microscopic examination at the Department of Pharmaceutical Botany, Faculty of Pharmacy, "Victor Babeș" University of Medicine and Pharmacy Timișoara, Romania [80]. The voucher is held in the university herbarium under accession JAA-01-23. Powdered cone berries

(300 g) were extracted with three 1 L portions of 99.5% ethanol (Riedel-de Haën/Fisher Scientific, Helsinki, Finland) with ultrasound assistance using an Elmasonic S120 ultrasonic bath (Elma Schmidbauer GmbH, Singen, Germany; 20 min per extraction). Concentration of the combined filtrates under reduced pressure using a Laborota 4000eco rotary evaporator (Heidolph Instruments GmbH & Co. KG, Schwabach, Germany) yielded 56.69 g (18.90%, *w*/*w*) of crude extract. A 20 g portion was suspended in 100 mL of distilled water and partitioned successively with petroleum ether, diethyl ether, ethyl acetate and water-saturated *n*-butanol (three 150 mL portions of each solvent). This yielded F1 (crude ethanolic extract), F2 (petroleum ether), F3 (diethyl ether), F4 (ethyl acetate), F5 (*n*-butanol) and F6 (residual aqueous). The preparations originated from the experimental batch used in the earlier work [26,27]. The published HPLC–MS profiles for F1, F3, F4 and F5 informed interpretation [26–28]. Ethanol was used instead of methanol because of its lower toxicity and to obtain the parent extract for comparison with the previously characterised fractions [26,27].

Dry preparations were dissolved in DMSO and brought to 4 mg/mL with PBS. The nominal calculation uses approximately 300 µL of DMSO in 4.0 mL of working solution. In a final incubation volume of 2.0 mL, addition of 5, 50 or 500 µL yielded preparation concentrations of 10, 100 or 1000 µg/mL and estimated DMSO levels of 0.01875%, 0.1875% or 1.875% (*v*/*v*), respectively.

4.3. HSA Glycation

Reaction mixtures were prepared by combining 1.0 mL of HSA stock solution (80 mg/mL in PBS, pH 7.4) with the appropriate amounts of glucose and extract or fractions, followed by adjustment to a final volume of 2.0 mL with PBS. The final concentrations were 40 mg/mL for HSA, 30 or 300 mM for glucose, and 10, 100, or 1000 µg/mL for the extract or fractions. Sodium azide was present at a final concentration of 0.1%.

Controls comprised HSA in PBS, HSA with glucose in PBS and corresponding incubations containing 1 mM aminoguanidine. Each preparation was also incubated with HSA without glucose to measure the sample background. Samples were incubated for 28 days at 37 °C with shaking at 50 rpm using an Incubator 1000 and a Polymax 1040 (Heidolph Instruments) and dialysed against PBS for 48 h. Each control and treatment was prepared in three independent tubes ($n = 3$).

4.4. Protein Determination and Normalisation

After dialysis, HSA was estimated from absorbance at 280 nm measured on a SPECORD 50 PLUS spectrophotometer (Analytik Jena, Jena, Germany), using a 1 cm cuvette and a mass absorption coefficient of 0.55 mL mg^{-1} cm^{-1}. For this optical path, HSA (mg/mL) = A_{280} × dilution factor/0.55. The primary figures and Tables S1A and S1B retain the recorded protein-adjusted readouts and their within-incubation treatment/control ratios. A separate A_{280}-based sensitivity analysis is presented for F4 at 30 mM glucose in Table S2. The assignment of the retained A_{280} blocks to incubations is provisional: two blocks carry the same series label, although the first block matches the separate first-incubation record. This reconstruction therefore does not establish a corrected set of primary results.

Fructosamine (nmol/mg protein) is calculated as 1000 × concentration (mmol/L)/HSA (mg/mL), and CML (ng/mg protein) as concentration (ng/mL)/HSA (mg/mL). A common sample-specific protein denominator could not be verified for all recorded endpoints. Under the provisional assignment used in Table S2, the 30 mM glucose control in incubation 2 gives 37.97 nmol/mg fructosamine, compared with the recorded 52.00 nmol/mg. This discrepancy cannot be attributed to a calculation error without confirming sample identity. The first-incubation fluorescence record documents scaling by the ratio of a reference HSA concentration (0.5445 mg/mL) to the HSA concentration of the diluted sample; the

dimensionless ratio retains fluorescence in AU. Later-incubation fluorescence comparisons use the recorded adjusted values. The reported scales are AU for fluorescence, nmol/mg protein for fructosamine and ng/mg protein for CML; uniform application of the same denominator across endpoints is not established.

4.5. Fructosamine

Fructosamine was determined colorimetrically by reduction of iodonitrotetrazolium chloride (INT), based on the alkaline INT reaction described by Rosenthal and Olenick [81] and adapted to 96-well plates using a Synergy HTX microplate reader (BioTek Instruments, Winooski, VT, USA). Samples and standards were pretreated with 0.1 M carbonate buffer containing 0.4 M NaOH, using a sample-to-preparation-reagent ratio of 10:1 (v/v), and held for 30 min at room temperature. The INT working reagent contained 0.57 mM INT in 0.1 M carbonate buffer (pH 10.35). Pretreated aliquots were mixed with the INT working reagent at a ratio of 1:20 (v/v), corresponding to a nominal final INT concentration of approximately 0.54 mM ($0.57 \times 20/21$). For each sample or standard, the matched blank contained the corresponding pretreated aliquot with carbonate buffer replacing the INT working reagent. Absorbance was recorded at 550 nm, and the 60 min endpoint was used for quantification. The corresponding blank absorbance was subtracted before technical wells were averaged. The calibrator was 1-deoxy-1-morpholino-D-fructose (Sigma-Aldrich, D6149, CAS 6291-16-3). Standards and samples underwent the same preparation and analytical procedure. The calibration range was 0–10 mmol/L before protein adjustment; estimates above the highest calibrator were obtained by extrapolation and interpreted descriptively (Sections 2.2 and 3.4). Results are reported on the recorded nmol/mg protein scale (Section 4.4).

4.6. AGE-Associated Fluorescence

Dialysed samples were diluted in PBS and measured in a quartz cuvette on an LS50B luminescence spectrometer (PerkinElmer, Waltham, MA, USA) with 5-nm excitation and emission slits. Fluorescence was recorded in two channels [31,33,34]. At 335 nm excitation, the compiled data label the emission as 385 nm, and the first-incubation worksheet lists 380 nm. The acquisition record needed to establish the emission setting was unavailable. Figures and supplementary column headings retain the compiled label. The second channel used 370 nm excitation and 440 nm emission. Relative responses were calculated within each incubation from the recorded protein-adjusted signals (Section 4.4).

4.7. CML Immunoassay

CML was measured by competitive ELISA using kit ELK7896 (ELK Biotechnology, Wuhan, China) according to the manufacturer's instructions. Each well received 50 µL of undiluted dialysed sample (sample dilution factor 1). Absorbance was read at 450 nm with a 570 nm reference. The calibration series comprised 0, 78.13, 156.25, 312.5, 625, 1250, 2500 and 5000 ng/mL. The manufacturer specifies a measurement range of 78.13–5000 ng/mL [82]. Sample concentrations were calculated from a four-parameter logistic (4PL) calibration curve. Results are reported on the recorded ng/mg protein scale (Section 4.4). The author-confirmed 300 mM CML control summary is 80.08 ± 5.09 ng/mg protein (Table 1). Its underlying control triplet could not be matched to that used for Figure 1D. Table 1 and Figure 1D are therefore separate descriptive summaries and must not be combined to derive absolute treatment concentrations. The relative CML responses are exploratory and do not establish a quantitative antiglycation effect.

4.8. Data Handling

The independent incubation tube was the experimental unit. Technical well readings were averaged within a tube. Arithmetic means and sample SDs ($n - 1$) were calculated across the three independent values for each complete group. Concentrations were treated as separate conditions.

For each independent incubation, the relative response (%) was calculated as 100 × the recorded protein-adjusted treatment value divided by its corresponding glucose control. The mean and sample SD were then calculated across the three within-incubation percentages. The main response plots express the recorded response as a percentage of the glucose control (100%), whereas the corresponding supplementary results tables express the percentage reduction, calculated as 100 minus the relative response. Thus, the plotted response and the tabulated reduction are complementary percentage measures. Preparation-containing no-glucose backgrounds were not subtracted in these main response comparisons.

For Figure S1, matched background subtraction was performed separately within each incubation. The treatment reading obtained with glucose was corrected by subtracting the corresponding HSA–preparation reading obtained without glucose; the glucose-control reading was corrected by subtracting HSA alone without glucose. A percentage reduction was calculated from these two net signals for each incubation, and the percentages were then averaged across the three incubations. All endpoints had been adjusted for protein before background subtraction. Comparisons without a complete no-glucose triplet (NA in Figure 3) are marked NA in Figure S1. The F4 fructosamine ratios at 300 mM glucose were also examined in each incubation separately (Table S1B).

Calculations were performed using Python (version 3.12.14), and figures were prepared using Matplotlib (version 3.11.2). Spectra Manager (version 2.5; JASCO Corporation, Hachioji, Japan) was used for fluorescence data processing.

5. Conclusions

At 30 mM glucose, F3 showed a concentration-related decrease in the protein-normalized fructosamine response, whereas F4 showed its largest decreases at 10 and 100 µg/mL. These patterns identify F3 and F4 for further evaluation of early HSA glycation under this glucose condition. The lower CML responses of F2 at 30 mM glucose provide a separate exploratory finding. Published phytochemical profiles identify plausible contributors to the F3 and F4 responses, but do not establish constituent-specific mechanisms. Fluorescence decreases cannot be equated with inhibition of AGE formation. The next step is to verify these responses with vehicle-matched controls and an independent measurement of a defined glycation product. Fractions with confirmed activity can then be assessed in ocular models to guide the selection of a candidate for ophthalmic formulation development, physicochemical characterisation and biological evaluation.

Supplementary Materials: The following supporting information can be downloaded at: https://www.mdpi.com/article/10.3390/molecules31234318/s1, Table S1A. Percentage reductions relative to the glucose control at 30 mM glucose; Table S1B. Reductions relative to the glucose control at 300 mM glucose; Table S2. Protein estimates and fructosamine values for F4 and its controls at 30 mM glucose; Figure S1 (Section S2). Sensitivity of assay responses to matched-background subtraction.

Author Contributions: Conceptualization, A.D.-J.; methodology, A.D.-J.; software, A.D.-J.; validation, A.D.-J.; formal analysis, A.D.-J.; investigation, A.D.-J., A.A.J., K.W., M.G. and E.Ż.-P.; resources, A.D.-J. and A.A.J.; data curation, A.D.-J.; writing—original draft preparation, A.D.-J.; writing—review and editing, A.D.-J., D.-S.T.-A., B.K. and E.Ż.-P.; visualization, A.D.-J.; supervision, A.D.-J.; project administration, A.D.-J.; funding acquisition, A.D.-J. A.A.J. prepared and supplied the plant extract and fractions. K.W. and M.G. contributed to experimental AGE measurements. All authors have read and agreed to the published version of the manuscript.

Funding: This research was funded by Wroclaw Medical University under project No. IDUB.D190.24.024.

Institutional Review Board Statement: Not applicable.

Informed Consent Statement: Not applicable.

Data Availability Statement: The data supporting the findings of this study are included in the article and its Supplementary Materials. Raw assay records are available from the corresponding author on request.

Acknowledgments: The authors used OpenAI Codex (OpenAI, GPT-6) for language editing, manuscript revision and preparation of analysis and figure code. The documented scripts were used for numerical analyses and figure preparation. The authors are responsible for the final content.

Conflicts of Interest: The authors declare no conflicts of interest. The funder had no role in the design of the study; in the collection, analyses, or interpretation of data; in the writing of the manuscript; or in the decision to publish the results.

Abbreviations

AGE, advanced glycation end product; AG, aminoguanidine; BSA, bovine serum albumin; CML, N^{ε}-(carboxymethyl)lysine; DMSO, dimethyl sulfoxide; HPLC–MS, high-performance liquid chromatography–mass spectrometry; HSA, human serum albumin; INT, iodonitrotetrazolium chloride; NBT, nitroblue tetrazolium chloride; PBS, phosphate-buffered saline; RAGE, receptor for advanced glycation end products; SD, standard deviation.

References

1. Singh, R.; Barden, A.; Mori, T.; Beilin, L. Advanced Glycation End-Products: A Review. *Diabetologia* **2001**, *44*, 129–146. Erratum in *Diabetologia* **2002**, *45*, 293. [CrossRef] [PubMed]
2. Bucala, R.; Cerami, A. Advanced Glycosylation: Chemistry, Biology, and Implications for Diabetes and Aging. *Adv. Pharmacol.* **1992**, *23*, 1–34. [CrossRef] [PubMed]
3. Rabbani, N.; Thornalley, P.J. Dicarbonyl Stress in Cell and Tissue Dysfunction Contributing to Ageing and Disease. *Biochem. Biophys. Res. Commun.* **2015**, *458*, 221–226. [CrossRef] [PubMed]
4. Schalkwijk, C.G.; Stehouwer, C.D.A. Methylglyoxal, a Highly Reactive Dicarbonyl Compound, in Diabetes, Its Vascular Complications, and Other Age-Related Diseases. *Physiol. Rev.* **2020**, *100*, 407–461. [CrossRef] [PubMed]
5. Twarda-Clapa, A.; Olczak, A.; Białkowska, A.M.; Koziołkiewicz, M. Advanced Glycation End-Products (AGEs): Formation, Chemistry, Classification, Receptors, and Diseases Related to AGEs. *Cells* **2022**, *11*, 1312. [CrossRef] [PubMed]
6. Khalid, M.; Petroianu, G.; Adem, A. Advanced Glycation End Products and Diabetes Mellitus: Mechanisms and Perspectives. *Biomolecules* **2022**, *12*, 542. [CrossRef] [PubMed]
7. Wu, X.Q.; Zhang, D.D.; Wang, Y.N.; Tan, Y.Q.; Yu, X.Y.; Zhao, Y.Y. AGE/RAGE in diabetic kidney disease and ageing kidney. *Free Radic. Biol. Med.* **2021**, *171*, 260–271. [CrossRef] [PubMed]
8. Dimitropoulos, A.; Rosado, C.J.; Thomas, M.C. Dicarbonyl-mediated AGEing and diabetic kidney disease. *J. Nephrol.* **2020**, *33*, 909–915. [CrossRef] [PubMed]
9. Tezel, G.; Luo, C.; Yang, X. Accelerated aging in glaucoma: Immunohistochemical assessment of advanced glycation end products in the human retina and optic nerve head. *Investig. Ophthalmol. Vis. Sci.* **2007**, *48*, 1201–1211. [CrossRef] [PubMed]
10. Park, C.H.; Kim, J.W. Effect of advanced glycation end products on oxidative stress and senescence of trabecular meshwork cells. *Korean J. Ophthalmol.* **2012**, *26*, 123–131. [CrossRef] [PubMed]
11. Wiglusz, K.; Żurawska-Płaksej, E.; Rorbach-Dolata, A.; Piwowar, A. How Does Glycation Affect Binding Parameters of the Albumin–Gliclazide System in the Presence of Drugs Commonly Used in Diabetes? In Vitro Spectroscopic Study. *Molecules* **2021**, *26*, 3869. [CrossRef] [PubMed]
12. Uzelac, T.; Smiljanić, K.; Takić, M.; Šarac, I.; Oggiano, G.; Nikolić, M.; Jovanović, V. The Thiol Group Reactivity and the Antioxidant Property of Human Serum Albumin Are Controlled by the Joint Action of Fatty Acids and Glucose Binding. *Int. J. Mol. Sci.* **2024**, *25*, 2335. [CrossRef] [PubMed]
13. Croes, C.A.C.C.; Chrysanthou, M.; Hoppenbrouwers, T.; Wichers, H.; Keijer, J.; Savelkoul, H.F.J.; Teodorowicz, M. Diabetic Glycation of Human Serum Albumin Affects Its Immunogenicity. *Biomolecules* **2024**, *14*, 1492. [CrossRef] [PubMed]
14. Velichkova, S.; Foubert, K.; Pieters, L. Natural Products as a Source of Inspiration for Novel Inhibitors of Advanced Glycation Endproducts (AGEs) Formation. *Planta Med.* **2021**, *87*, 780–801. Correction in *Planta Med.* **2021**, *87*, E5. [CrossRef] [PubMed]

15. Yeh, W.J.; Hsia, S.M.; Lee, W.H.; Wu, C.H. Polyphenols with antiglycation activity and mechanisms of action: A review of recent findings. *J. Food Drug Anal.* **2017**, *25*, 84–92. [CrossRef] [PubMed]
16. Asgharpour Dil, F.; Ranjkesh, Z.; Goodarzi, M.T. A systematic review of antiglycation medicinal plants. *Diabetes Metab. Syndr.* **2019**, *13*, 1225–1229. Erratum in *Diabetes Metab. Syndr.* **2021**, *15*, 475. [CrossRef] [PubMed]
17. Liu, Y.; Lu, L.; Yuan, S.; Guo, Y.; Yao, W.; Zhou, W.; Yu, H. Formation of advanced glycation end-products and α-dicarbonyl compounds through Maillard reaction: Solutions from natural polyphenols. *J. Food Compos. Anal.* **2023**, *120*, 105350. [CrossRef]
18. Maisto, M.; Tenore, G.C. Polyphenols as a Useful Tool to Ameliorate Advanced Glycation End-product Formation: A Focus on Molecular Mechanisms of Action. *Front. Biosci.-Landmark* **2024**, *29*, 424. [CrossRef] [PubMed]
19. Fecka, I.; Bednarska, K.; Kowalczyk, A. In Vitro Antiglycation and Methylglyoxal Trapping Effect of Peppermint Leaf (Mentha × piperita L.) and Its Polyphenols. *Molecules* **2023**, *28*, 2865. [CrossRef] [PubMed]
20. Thilavech, T.; Marnpae, M.; Mäkynen, K.; Adisakwattana, S. Phytochemical Composition, Antiglycation, Antioxidant Activity and Methylglyoxal-Trapping Action of Brassica Vegetables. *Plant Foods Hum. Nutr.* **2021**, *76*, 340–346. [CrossRef] [PubMed]
21. Sun, Y.; Xie, W.; Huang, Y.; Chen, X. Coffee leaf extract inhibits advanced glycation end products and their precursors: A mechanistic study. *J. Food Sci.* **2024**, *89*, 3455–3468. [CrossRef] [PubMed]
22. Miceli, N.; Trovato, A.; Dugo, P.; Cacciola, F.; Donato, P.; Marino, A.; Bellinghieri, V.; La Barbera, T.M.; Güvenç, A.; Taviano, M.F. Comparative Analysis of Flavonoid Profile, Antioxidant and Antimicrobial Activity of the Berries of *Juniperus communis* L. var. communis and *Juniperus communis* L. var. saxatilis Pall. from Turkey. *J. Agric. Food Chem.* **2009**, *57*, 6570–6577. [CrossRef] [PubMed]
23. Bais, S.; Gill, N.S.; Rana, N.; Shandil, S. A Phytopharmacological Review on a Medicinal Plant: *Juniperus communis*. *Int. Sch. Res. Not.* **2014**, *2014*, 634723. [CrossRef] [PubMed]
24. Belov, T.; Terenzhev, D.; Bushmeleva, K.N.; Davydova, L.; Burkin, K.; Fitsev, I.; Gatiyatullina, A.; Egorova, A.; Nikitin, E. Comparative Analysis of Chemical Profile and Biological Activity of *Juniperus communis* L. Berry Extracts. *Plants* **2023**, *12*, 3401. [CrossRef] [PubMed]
25. Gonçalves, A.; Flores-Félix, J.; Coutinho, P.; Alves, G.; Silva, L. Zimbro (*Juniperus communis* L.) as a Promising Source of Bioactive Compounds and Biomedical Activities: A Review on Recent Trends. *Int. J. Mol. Sci.* **2022**, *23*, 3197. [CrossRef] [PubMed]
26. Dan, C.; Almajan-Guta, B.; Jojić, A.A.; Dumitrel, S.I.; Predescu, I.A.; Tchiakpe-Antal, D.S.; Smeu, A.; Jijie, R.; Ionita, I.; Dragomir, A.C.; et al. Ethanolic Extract of *Juniperus communis* Exhibits Antimicrobial Activity and Selective Cytotoxicity in Panc-1 Cancer Cells Compared to HepaRG Hepatocytes. *Farmacia* **2025**, *73*, 362–375. [CrossRef]
27. Jojić, A.A.; Pașcalau, N.A.; Antal, A.G.; Uţu, D.; Muntean, D.; Vlase, L.; Vlase, A.M.; Moacă, E.A.; Ruse, G.; Bihoi-Rădoi, L.; et al. Fraction-Dependent Polyphenolic Profile and Biological Activities of *Juniperus communis* Pseudo-Fruit Extracts: Antioxidant, Antimicrobial and Selective Antimelanoma Effects. *Antioxidants* **2026**, *15*, 738. [CrossRef] [PubMed]
28. Jojić, A.A.; Uţu, D.; Antal, G.; Mioc, A.; Muntean, D.; Vlase, L.; Vlase, A.M.; Moacă, E.A.; Vodă, R.; Şoica, C.M.; et al. Polyphenol Profiling, Antibacterial Activity, and In Vitro Cytotoxic Effects of a Diethyl Ether Fraction from Juniper Cone Berries. *Molecules* **2026**, *31*, 3910. [CrossRef] [PubMed]
29. Asgary, S.; Naderi, G.A.; Shams Ardekani, M.R.; Sahebkar, A.; Airin, A.; Aslani, S.; Kasher, T.; Emami, S.A. Inhibition of Protein Glycation by Essential Oils of Branchlets and Fruits of *Juniperus communis* subsp. hemisphaerica. *Res. Pharm. Sci.* **2014**, *9*, 179–185. [PubMed]
30. Arasteh, A.; Farahi, S.; Habibi-Rezaei, M.; Moosavi-Movahedi, A.A. Glycated Albumin: An Overview of the In Vitro Models of an In Vivo Potential Disease Marker. *J. Diabetes Metab. Disord.* **2014**, *13*, 49. [CrossRef] [PubMed]
31. Schmitt, A.; Schmitt, J.; Münch, G.; Gasic-Milencovic, J. Characterization of Advanced Glycation End Products for Biochemical Studies: Side Chain Modifications and Fluorescence Characteristics. *Anal. Biochem.* **2005**, *338*, 201–215. [CrossRef] [PubMed]
32. Johnson, R.N.; Metcalf, P.A.; Baker, J.R. Fructosamine: A New Approach to the Estimation of Serum Glycosylprotein. An Index of Diabetic Control. *Clin. Chim. Acta* **1983**, *127*, 87–95. [CrossRef] [PubMed]
33. Münch, G.; Keis, R.; Wessels, A.; Riederer, P.; Bahner, U.; Heidland, A.; Niwa, T.; Lemke, H.D.; Schinzel, R. Determination of Advanced Glycation End Products in Serum by Fluorescence Spectroscopy and Competitive ELISA. *Clin. Chem. Lab. Med.* **1997**, *35*, 669–677. [CrossRef] [PubMed]
34. Wu, J.T.; Tu, M.C.; Zhung, P. Advanced Glycation End Product (AGE): Characterization of the Products from the Reaction between D-Glucose and Serum Albumin. *J. Clin. Lab. Anal.* **1996**, *10*, 21–34. [CrossRef]
35. Ahmed, M.U.; Thorpe, S.R.; Baynes, J.W. Identification of Nε-(Carboxymethyl)lysine as a Degradation Product of Fructoselysine in Glycated Protein. *J. Biol. Chem.* **1986**, *261*, 4889–4894. [CrossRef]
36. Fu, M.X.; Requena, J.R.; Jenkins, A.J.; Lyons, T.J.; Baynes, J.W.; Thorpe, S.R. The Advanced Glycation End Product, Nε-(Carboxymethyl)lysine, Is a Product of Both Lipid Peroxidation and Glycoxidation Reactions. *J. Biol. Chem.* **1996**, *271*, 9982–9986. [CrossRef] [PubMed]

37. Delgado-Andrade, C. Carboxymethyl-Lysine: Thirty Years of Investigation in the Field of AGE Formation. *Food Funct.* **2016**, *7*, 46–57. [CrossRef] [PubMed]
38. Ishikawa, M.; Taniguchi, R.; Taniguchi, T.; Yang, Z.; Nishikata, T. Re-evaluation of the antiglycation activity of herbal extracts using multiple antiglycation assays. *Biosci. Biotechnol. Biochem.* **2026**, *90*, 1482–1489. [CrossRef] [PubMed]
39. Séro, L.; Sanguinet, L.; Blanchard, P.; Dang, B.T.; Morel, S.; Richomme, P.; Séraphin, D.; Derbré, S. Tuning a 96-Well Microtiter Plate Fluorescence-Based Assay to Identify AGE Inhibitors in Crude Plant Extracts. *Molecules* **2013**, *18*, 14320–14339. [CrossRef] [PubMed]
40. Usacheva, T.; Gamov, G.; Bychkova, A.; Anufrikov, Y.; Shasherina, A.; Alister, D.; Kuranova, N.; Sharnin, V. Binding of quercetin and curcumin to human serum albumin in aqueous dimethyl sulfoxide and in aqueous ethanol. *J. Therm. Anal. Calorim.* **2022**, *147*, 5511–5518. [CrossRef] [PubMed]
41. Thornalley, P.J. Use of Aminoguanidine (Pimagedine) to Prevent the Formation of Advanced Glycation Endproducts. *Arch. Biochem. Biophys.* **2003**, *419*, 31–40. [CrossRef] [PubMed]
42. Dołowacka-Jóźwiak, A.; Matkowski, A.; Nawrot-Hadzik, I. Antiglycoxidative Properties of Extracts and Fractions from *Reynoutria* Rhizomes. *Nutrients* **2021**, *13*, 4066. [CrossRef] [PubMed]
43. Ali, M.Y.; Zamponi, G.W.; Abdul, Q.A.; Seong, S.H.; Min, B.S.; Jung, H.A.; Choi, J.S. Prunin from *Poncirus trifoliata* (L.) Rafin Inhibits Aldose Reductase and Glucose-Fructose-Mediated Protein Glycation and Oxidation of Human Serum Albumin. *J. Agric. Food Chem.* **2024**, *72*, 7203–7218. [CrossRef] [PubMed]
44. Bernacka, K.; Bednarska, K.; Starzec, A.; Mazurek, S.; Fecka, I. Antioxidant and Antiglycation Effects of *Cistus* × *incanus* Water Infusion, Its Phenolic Components, and Respective Metabolites. *Molecules* **2022**, *27*, 2432. [CrossRef] [PubMed]
45. Zhang, L.; Zhou, Q.M.; Xu, L.; Xie, X.; Wang, P.X.; Xie, Z.H.; Li, J.L.; Tu, Z.C. Extraction optimization and identification of four advanced glycation-end products inhibitors from lotus leaves and interaction mechanism analysis. *Food Chem.* **2023**, *414*, 135712. [CrossRef] [PubMed]
46. Liu, J.; Yang, Z.; Cheng, Y.; Wu, Q.; He, Y.; Li, Q.; Cao, X. Eriodictyol and Naringenin Inhibit the Formation of AGEs: An In Vitro and Molecular Interaction Study. *J. Mol. Recognit.* **2020**, *33*, e2814. [CrossRef] [PubMed]
47. Lee, E.H.; Song, D.G.; Lee, J.Y.; Pan, C.H.; Um, B.H.; Jung, S.H. Inhibitory Effect of the Compounds Isolated from Rhus verniciflua on Aldose Reductase and Advanced Glycation Endproducts. *Biol. Pharm. Bull.* **2008**, *31*, 1626–1630. [CrossRef] [PubMed]
48. Ma, T.X.; Zhang, L.; Xu, L.; Ye, Y.H.; Huang, T.; Zhou, Q.M.; Liu, H.L. Mitigation of isoquercitrin on β-lactoglobulin glycation: Insight into the mechanisms by mass spectrometry and interaction analysis. *Int. J. Biol. Macromol.* **2020**, *155*, 1133–1141. [CrossRef] [PubMed]
49. Zhang, L.; Xu, L.; Tu, Z.C.; Wang, H.H.; Luo, J.; Ma, T.X. Mechanisms of isoquercitrin attenuates ovalbumin glycation: Investigation by spectroscopy, spectrometry and molecular docking. *Food Chem.* **2020**, *309*, 125667. [CrossRef] [PubMed]
50. Mukai, R.; Okuyama, H.; Uchimura, M.; Sakao, K.; Matsuhiro, M.; Ikeda-Imafuku, M.; Ishima, Y.; Nishikawa, M.; Ikushiro, S.; Tai, A. The binding selectivity of quercetin and its structure-related polyphenols to human serum albumin using a fluorescent dye cocktail for multiplex drug-site mapping. *Bioorg. Chem.* **2024**, *145*, 107184. [CrossRef] [PubMed]
51. Zhou, Q.; Cheng, K.W.; Gong, J.; Li, E.T.; Wang, M. Apigenin and Its Methylglyoxal-Adduct Inhibit Advanced Glycation End Products-Induced Oxidative Stress and Inflammation in Endothelial Cells. *Biochem. Pharmacol.* **2019**, *166*, 231–241. [CrossRef] [PubMed]
52. Sarmah, S.; Das, S.; Roy, A.S. Protective Actions of Bioactive Flavonoids Chrysin and Luteolin on the Glyoxal Induced Formation of Advanced Glycation End Products and Aggregation of Human Serum Albumin: In Vitro and Molecular Docking Analysis. *Int. J. Biol. Macromol.* **2020**, *165*, 2275–2285. [CrossRef] [PubMed]
53. Kontogianni, V.G.; Charisiadis, P.; Margianni, E.; Lamari, F.N.; Gerothanassis, I.P.; Tzakos, A.G. Olive Leaf Extracts Are a Natural Source of Advanced Glycation End Product Inhibitors. *J. Med. Food* **2013**, *16*, 817–822. [CrossRef] [PubMed]
54. Grzegorczyk-Karolak, I.; Gołąb, K.; Gburek, J.; Wysokińska, H.; Matkowski, A. Inhibition of Advanced Glycation End-Product Formation and Antioxidant Activity by Extracts and Polyphenols from *Scutellaria alpina* L. and *S. altissima* L. *Molecules* **2016**, *21*, 739. [CrossRef] [PubMed]
55. Tagliazucchi, D.; Martini, S.; Conte, A. Protocatechuic and 3,4-Dihydroxyphenylacetic Acids Inhibit Protein Glycation by Binding Lysine through a Metal-Catalyzed Oxidative Mechanism. *J. Agric. Food Chem.* **2019**, *67*, 7821–7831. [CrossRef] [PubMed]
56. Bhuiyan, M.N.I.; Mitsuhashi, S.; Sigetomi, K.; Ubukata, M. Quercetin inhibits advanced glycation end product formation via chelating metal ions, trapping methylglyoxal, and trapping reactive oxygen species. *Biosci. Biotechnol. Biochem.* **2017**, *81*, 882–890. [CrossRef]
57. Wu, C.-H.; Yen, G.-C. Inhibitory Effect of Naturally Occurring Flavonoids on the Formation of Advanced Glycation Endproducts. *J. Agric. Food Chem.* **2005**, *53*, 3167–3173. [CrossRef] [PubMed]

58. Mohammadpour, A.; Sadeghi, M.; Miroliaei, M. Role of Structural Peculiarities of Flavonoids in Suppressing AGEs Generated From HSA/Glucose System. *Appl. Biochem. Biotechnol.* **2024**, *196*, 6296–6314. [CrossRef] [PubMed]
59. Bednarska, K.; Fecka, I. Potential of Vasoprotectives to Inhibit Non-Enzymatic Protein Glycation, and Reactive Carbonyl and Oxygen Species Uptake. *Int. J. Mol. Sci.* **2021**, *22*, 10026. [CrossRef]
60. Thornalley, P.J. Protein and Nucleotide Damage by Glyoxal and Methylglyoxal in Physiological Systems—Role in Ageing and Disease. *Drug Metabol. Drug Interact.* **2008**, *23*, 125–150. [CrossRef]
61. Zhou, Y.; Duan, H.; Chen, J.; Ma, S.; Wang, M.; Zhou, X. The mechanism of in vitro non-enzymatic glycosylation inhibition by Tartary buckwheat's rutin and quercetin. *Food Chem.* **2023**, *406*, 134956. [CrossRef] [PubMed]
62. Wani, M.J.; Salman, K.A.; Hashmi, M.A.; Siddiqui, S.; Moin, S. Rutin impedes human low-density lipoprotein from non-enzymatic glycation: A mechanistic insight against diabetes-related disorders. *Int. J. Biol. Macromol.* **2023**, *238*, 124151. [CrossRef] [PubMed]
63. Stachelska, M.A.; Karpiński, P.; Kruszewski, B. A Comprehensive Review of Biological Properties of Flavonoids and Their Role in the Prevention of Metabolic, Cancer and Neurodegenerative Diseases. *Appl. Sci.* **2025**, *15*, 10840. [CrossRef]
64. Gulcin, İ. Antioxidants: A Comprehensive Review. *Arch. Toxicol.* **2025**, *99*, 1893–1997. [CrossRef] [PubMed]
65. Savini, F.; Bobone, S.; Stella, L.; Roversi, D.; Bocedi, A. Methods of Inner Filter Effect Correction in Fluorescence Measurements of Protein–Ligand Association: A Re-Examination of the Association of Anti-HIV Drugs to Serum Albumin. *Chem.–Methods* **2026**, *6*, e70094. [CrossRef]
66. Ou, P.; Wolff, S.P. Aminoguanidine: A Drug Proposed for Prophylaxis in Diabetes Inhibits Catalase and Generates Hydrogen Peroxide In Vitro. *Biochem. Pharmacol.* **1993**, *46*, 1139–1144. [CrossRef]
67. Skamarauskas, J.T.; McKay, A.G.; Hunt, J.V. Aminoguanidine and Its Pro-Oxidant Effects on an Experimental Model of Protein Glycation. *Free Radic. Biol. Med.* **1996**, *21*, 801–812. [CrossRef] [PubMed]
68. Soboleva, A.; Vikhnina, M.; Grishina, T.; Frolov, A. Probing Protein Glycation by Chromatography and Mass Spectrometry: Analysis of Glycation Adducts. *Int. J. Mol. Sci.* **2017**, *18*, 2557. [CrossRef] [PubMed]
69. Junho, C.V.C.; Dai, Y.; Schieren, L.; Hourtz, S.; Rykova, T.; Vondenhoff, S.; Wessiepe, M.; Zou, J.; Jankowski, J.; Goettsch, C.; et al. Advanced glycation end product (AGE)-modified albumin does not enhance neutrophil extracellular trap formation and minimally impacts endothelial inflammation in large vessels. *Life Sci.* **2026**, *398*, 124467. [CrossRef] [PubMed]
70. Zhang, Z.; Sethiel, M.S.; Shen, W.; Liao, S.; Zou, Y. Hyperoside Downregulates the Receptor for Advanced Glycation End Products (RAGE) and Promotes Proliferation in ECV304 Cells via the c-Jun N-Terminal Kinases (JNK) Pathway Following Stimulation by Advanced Glycation End-Products In Vitro. *Int. J. Mol. Sci.* **2013**, *14*, 22697–22707. [CrossRef] [PubMed]
71. Zhou, Q.; Xu, H.; Yu, W.; Li, E.; Wang, M. Anti-Inflammatory Effect of an Apigenin-Maillard Reaction Product in Macrophages and Macrophage-Endothelial Cocultures. *Oxid. Med. Cell. Longev.* **2019**, *2019*, 9026456. [CrossRef] [PubMed]
72. Tsai, S.J.; Yin, M.C. Anti-Glycative and Anti-Inflammatory Effects of Protocatechuic Acid in Brain of Mice Treated by D-Galactose. *Food Chem. Toxicol.* **2012**, *50*, 3198–3205. [CrossRef] [PubMed]
73. Wan, L.; Li, J.; Chen, W.B.; Wu, G.Q. Beneficial Effects of Protocatechuic Acid on Diabetic Retinopathy in Streptozocin-Induced Diabetic Rats. *Int. J. Ophthalmol.* **2023**, *16*, 855–862. [CrossRef] [PubMed]
74. Huang, R.; Zeng, J.; Yu, X.; Shi, Y.; Song, N.; Zhang, J.; Wang, P.; Luo, M.; Ma, Y.; Xiao, C.; et al. Luteolin Alleviates Diabetic Nephropathy Fibrosis Involving AMPK/NLRP3/TGF-β Pathway. *Diabetes Metab. Syndr. Obes.* **2024**, *17*, 2855–2867. [CrossRef]
75. Di Lorenzo, C.; Colombo, F.; Biella, S.; Stockley, C.; Restani, P. Polyphenols and Human Health: The Role of Bioavailability. *Nutrients* **2021**, *13*, 273. [CrossRef] [PubMed]
76. Teng, H.; Chen, L. Polyphenols and bioavailability: An update. *Crit. Rev. Food Sci. Nutr.* **2019**, *59*, 2040–2051. [CrossRef] [PubMed]
77. Xie, L.; Deng, Z.; Zhang, J.; Dong, H.; Wang, W.; Xing, B.; Liu, X. Comparison of Flavonoid O-Glycoside, C-Glycoside and Their Aglycones on Antioxidant Capacity and Metabolism during In Vitro Digestion and In Vivo. *Foods* **2022**, *11*, 882. [CrossRef] [PubMed]
78. Vaux, D.L.; Fidler, F.; Cumming, G. Replicates and repeats—What is the difference and is it significant? *EMBO Rep.* **2012**, *13*, 291–296. [CrossRef] [PubMed]
79. Grigoryan, K.R.; Shilajyan, H.A. Influence of Dimethylsulfoxide on the Fluorescence Behavior of Human Serum Albumin Studied by Excitation-Emission Matrix Fluorescence Spectroscopy Method. *Proc. YSU B Chem. Biol. Sci.* **2013**, *47*, 50–53. Available online: https://journals.ysu.am/proceedings-chem-biol/article/view/vol47_no1_2013_pp050-053 (accessed on 25 October 2026).
80. Jojić, A.A.; Semenescu, A.D.; Predescu, I.; Drăchici, G.A.; Muntean, D.; Ardelean, F.; Ruse, G.; Gogulescu, A.; Şoica, I.; Hegheş, A.; et al. Juniperi Galbulus: Screening of Phytochemicals and Bioactivity Investigation of the Aqueous Extract. *Farmacia* **2024**, *72*, 934–945. [CrossRef]

81. Rosenthal, M.A.; Olenick, L.J. Evaluation of a Single-Color-Reading Method for Determining Fructosamine. *Clin. Chem.* **1988**, *34*, 360–363. [CrossRef]
82. ELK Biotechnology. CML (Carboxymethyl Lysine) ELISA Kit, ELK7896: Instructions for Use. Available online: https://www.elk-biotech.com/upload/file/ELISA/ELK7896-1.pdf (accessed on 24 October 2026).

Disclaimer/Publisher's Note: The statements, opinions and data contained in all publications are solely those of the individual author(s) and contributor(s) and not of MDPI and/or the editor(s). MDPI and/or the editor(s) disclaim responsibility for any injury to people or property resulting from any ideas, methods, instructions or products referred to in the content.